Technical Report

# Design optimization of supports for overhanging structures in aluminum and titanium alloys by selective laser melting

F. Calignano *

Istituto Italiano di Tecnologia, Center for Space Human Robotics IIT@Polito, Corso Trento, 21, 10129 Torino, Italy

ABSTRACT

Selective laser melting (SLM) process allows fabricating strong, lightweight and complex metallic structures. To successfully produce metallic parts by SLM, additional structures are needed to support overhanging surfaces in order to dissipate process heat and to minimize geometrical distortions induced by internal stresses. However, these structures are often massive and require additional post-processing for their removal. A minimization of support structures would therefore significantly reduce manufacturing and finishing efforts and costs. This study investigates the manufacturability of overhanging structures using optimized support parts. An experimental study was performed to identify the optimal self-supporting overhanging structures using Taguchi $L_{36}$ design. Experimental results revealed that with optimized supports it is possible to build non-assembly mechanism with overhang surfaces. However, it is necessary to correctly orientate the part in the SLM machine in order to build it with a minimal support structure so to obtain the best trade-off between production time, cost, and accuracy.

© 2014 Elsevier Ltd. All rights reserved.

## 1. Introduction

Selective laser melting is an additive manufacturing (AM) process that enables the quick production of complex-shaped three-dimensional (3D) parts directly from metal powder [1,2]. In this process powdered materials are selectively fused by a focused laser beam in layer-by-layer fashion to obtain a near-net-shape product without the help of any binding material. Recent research efforts have demonstrated that SLM, due to its flexibility in feedstock and shapes, has a promising potential to manufacture cellular lattice structures with fine features, showing a great potential to make advanced lightweight structures and products which are highly desired by engineering sectors such as aerospace, automotive and medical industries [3–6]. Moreover, with the proper choice of input conditions, selective laser melting process can be used to build fully dense parts with mechanical properties equivalent or even superior to those of parts produced by conventional manufacturing. However, this process requires the presence of external support structures during the construction of a part. These structures are necessary to fix the part to the building platform, conduct excess heat away from the part and to prevent the warping and/or collapse. This can easily happen in the case of internal channels and when the amount of overhang exceeds a certain threshold value. However, the presence of support structures

increases both the time required for the part manufacturing and the time and complexity of post-processing operations. Minimizing the amount of supported surfaces can improve the process efficiency. Consequently, the geometrical design and optimization of the support structures are necessary to improve the sustainability and efficiency of metallic parts produced by SLM. One of the more effective ways to reduce the amount of support needed is to orientate the object into an optimal building position. In fact, depending on the object built orientation, the surface area of support structure changes sensitively. Allen and Dutta [7] described a method for determining the orientation for constructing an object with minimal support structures. In their algorithm, the best orientation is chosen from a list of the candidate orientations. If two orientations require support structures with equal surface areas of contact, the orientation in which the object has a lower centre of mass is chosen. Actually, it is unlikely that the two orientations would have a support structure with the same contact area. Frank and Fadel [8] proposed an expert system that considers surface finishing, build time, and support generation. The appropriate orientation is then selected from the surface finishing. Build time is estimated by roughly slicing the part. Strano et al. [9] presented a new approach to the design of support structures that optimize the part built orientation and the support cellular structure. The primary aim of the present investigation was studied, the optimal design of support structures in SLM process applying the Taguchi method [10–12], in order to improve the process efficiency and minimize manufacturing defects. To do this, it is necessary to

* Tel.: +39 0110903406.
E-mail address: flaviana.calignano@iit.it

analyze, first of all, the structures that are typically classified as critical during the building process, as the overhang structures. The samples were fabricated in AlSi10Mg and Ti6Al4V alloys, two of the most common employed metal materials for AM.

## 2. Overhanging and support structures

As mentioned above, to reduce the support structures, it is necessary to determine the optimal orientation of the part on the building platform. This can be done starting from the identification of critical geometries for the SLM process. These are generically called overhanging structures. In AM process, it is considered an overhanging structure (Fig. 1) a part of a component that is not supported during building, by solidified material or a substrate on the bottom side. Consequently, the melt pool created by the heat input from the laser is supported by powder material. From this definition, it is clear that whether a part of a component is an overhanging structure or not also depends on the orientation given to the part while building it (Fig. 1d). Therefore, analyzing the limits of construction of the overhanging structures, it is possible to determine the areas that require support structures and then derive the optimal orientation. In any building orientation, the part is defined with its base on the xy-plane and the building direction is along the z axis.

### 2.1. Fabricating defects

Unfortunately, overhanging structures cannot always be avoided. The main defects that frequently happen during their fabrication are staircase effect, dross formation and warp. SLM process starts with the creation of a three-dimensional CAD-model of an object. Then the model is converted to a STL file format. This file defines optimal building direction of the physical object and it is based on small triangles, which determine the accuracy and contours of the whole object. Then, the support structures are generated. Since the whole object is manufactured starting from a tessellation of a 3D CAD model, the contour of a SLM part is a stepped approximation of the contour of the nominal CAD model. As a result of this, all parts manufactured by AM processes exhibit a staircase effect (Fig. 2). The uniform slicing procedure directly affects the extent of the staircase effect that appears especially along inclined planes and curved surfaces. As the inclination angle is reduced or the layer thickness is increased, the stair effect becomes more pronounced. When the slicing thickness is thinner, the staircase is smaller and the surface will be smoother.

As shown in Fig. 3 (region a), when laser irradiates solid-supported zones, the heat conduction rate is high. Instead, when laser irradiates powder-supported zones (region b), the heat conduction rate is much lower than the solid-supported zone [13]. This situation often happens during overhanging surface fabrication. Therefore, the absorbed energy input will be much higher when laser
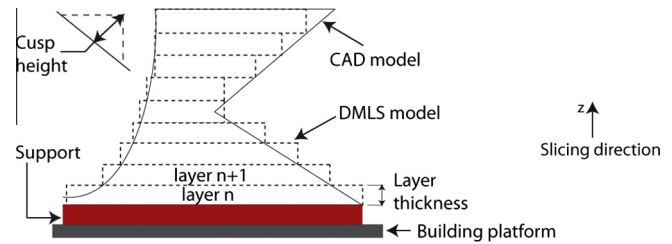


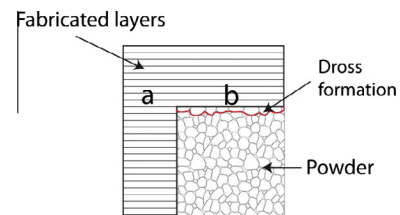**Fig. 2.** Staircase effect on the DMLS model.



**Fig. 3.** Dross formation on overhanging surface.

irradiates powder-supported zones, and this leads the melt pool to become too large and to sink into the powder as the result of gravity and capillary forces. For the above reason, dross will be formed and dimensional accuracy is likely to be lower during SLM fabrication of overhanging surfaces.

Warping defect (Fig. 4) is another effect not negligible, which is due to the thermal stresses caused by rapid solidification during SLM process [14]. When the thermal stress exceeds the strength of the material, then plastic deformation occurs. The warping defect of an overhanging surface is also due to the lack of supports to secure the layer with the previous layers or to the few supports used.

### 2.2. Support structures

As illustrated in Fig. 5, the external support structure A is used to prevent surface $F_1$ from dropping, where $F_1$ is an overhanging surface. Structure B is used to prop up the overhanging surface $F_2$ because the initial layers of $F_2$ during its fabrication are not attached to the main body. At the same time, support structure B can prevent the part to deform during fabrication.

A support structure may be decomposed into two functional areas: teeth, connections between the main support and the part thus minimizing the contact area, and the main support structure (Fig. 6a). Adding teeth greatly eases support removal and ensures a better surface quality. However, teeth too close imply greater difficulty in removal of the part. Teeth too far can lead to a greater deformation of the part.
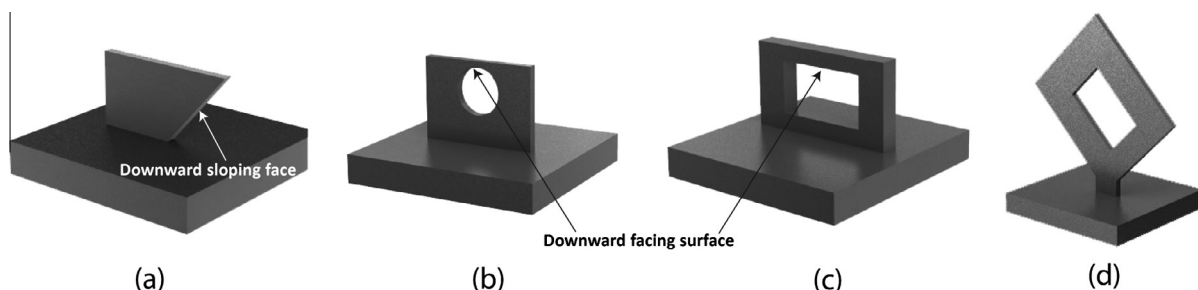


**Fig. 1.** Example of overhanging structures: (a) downward sloping face, (b) and (c) downward facing surfaces and (d) downward sloping faces obtained by orientation in the building platform.
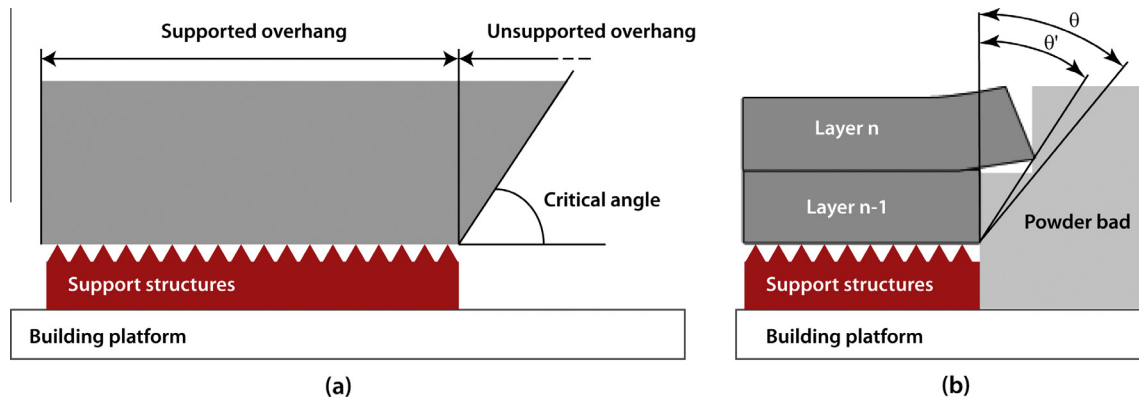
Fig. 4. (a) Supported and unsupported overhang structures and (b) Warping principle in the unsupported structure: the effective inclined angle $\theta'$ between the overhanging part of the layer under consideration and the previous layer was smaller than the designed inclined angle $\theta$.
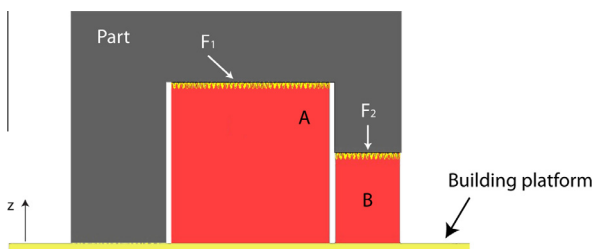


Fig. 5. Example of support structures: solid supported zone (region A) and powder supported zone (region B).
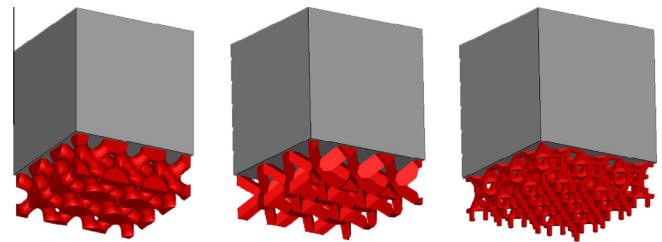


Fig. 7. Examples of different types of lattice support structures.

The main support should be strong enough to withstand both the vertical weight and other horizontal disturbances [15]. For this reason, generally a support structure called block is used. The block supports are rather applied for volumetric massive parts. They are made with a grid of $x$ and $y$ lines separated at a certain distance ($x$ hatching and $y$ hatching). Hatching can be chosen depending on the surface area. When creating block supports, it is convenient to fragment the block. Fragmentation will leave a small gap in the hatching of the block support at each chosen distance, so the removal of block supports will become a lot easier. Fig. 6b shows different support geometries mainly used for stereolithography, selective laser sintering and selective laser melting. A point support is used for very small features, a web support for circular areas and a line support for narrow down facing areas. Contour support is used to better sustain the contours of the parts in metal sintering.

To further the ease in removing supports, they can be perforated with diamond or rectangular shapes [16,17], or it is possible to implement lattice support structures design by combining a number of basic cell elements (Fig. 7).

These structures show good manufacturability characteristics even though some of the parts fail during the build because the struts of the structures connecting them are very thin. This fact is due to a low percentage of volume fraction, which is too fragile to be consistently manufactured with SLM process. Furthermore, for big cell sizes, the distance between the adjacent contact points to the supported surface is too large; therefore, there is too much unsupported material and the part is distorted by thermal stresses. Many factors have to be considered during design and manufacturing of more efficient lattice support structures. A compromise has to be reached between the best combination of cell size and volume fraction that is manufacturable, fast to build, easy to remove and which shows good thermal and mechanical properties to constrain deformation while ensuring reliable build for the part [18].

## 3. Experimental methods

### 3.1. Experimental design

Experimental design is the process of planning a study to meet specified objectives. Planning an experiment properly is very important in order to ensure that the right type of data. One of the main goals of a designed experiment is to partition the effects
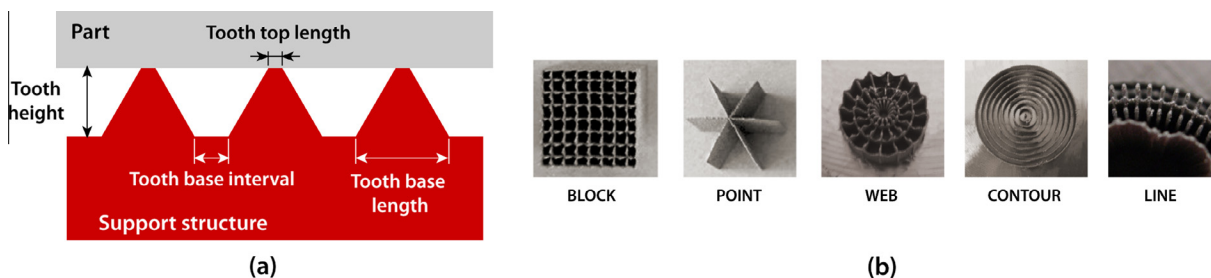


Fig. 6. (a) Description of the support structure and (b) examples of different types of support structures.

of the sources of variability into distinct components in order to examine specific questions of interest. The objective of designed experiments is to improve the precision of the results in order to verify the research hypotheses. Therefore, the experimental analysis was started from the identification of the self-supporting overhang structures. Once highlighted the limits of construction without the use of supports on some surfaces, it was studied the geometry of the supports in order to make easier the removal of parts from the building platform and reduce, if not eliminating, the problems of deformation due to a bad anchoring of the part on the platform. A non-assembly mechanism was used to verify if the support structures optimized to allow the fabrication of the part overcoming the problem of the overhang structures and the ease of removal of the part from the platform. A non-assembly mechanism is one-step fabrication of multi-articulated systems without requiring assembly of their structural members and joints after fabrication [19,20].

### 3.1.1. Self-supporting surfaces

Self-supporting angle is used to control the creation of supports on angled walls and surfaces. It represents the minimum angle of the part wall that will be built without supports. Facets that are closer to flat and having an inclination less than the self-supporting angle will be built on tops of supports. Four types of overhanging structures were investigated: downward sloping face, concave and convex radii, ledge (Fig. 8). Due to high thermal stresses typical of the SLM process, which can cause deformation of the part, downward sloping faces with angles smaller than 45° (angle between the *xy*-plane and the face) have to be supported. It is well known in literature [21–24] that for angles greater than 45°, they are self-supporting and the values of surface roughness decreases with increasing angle because the staircase effect is reduced. Oh the other hand, angles smaller than 30° lead to an increase in the staircase effect. For this reason, a range between 30° and 45° was chosen, with incremental steps of 5°. The concave radii test was designed to identify the limitations of building concave radii on part accuracy when making both tangential and partially tangential radii, and it identified the critical dimensions that need to be considered to make self-supporting radii. The tangent of a concave radius varies and is smallest at the top of the radius curve. Convex radii are fundamental in the construction of holes and channels, blend sharp external corners and for complex curved surfaces. A typical convex radii curve has a varied tangent that causes the base of the radii curve to become overhanging. This test investigated the effect on part accuracy in the same way as concave radii. Based on the analysis of the benchmarks in literature [21–24], concave and convex radii tests were designed with overhanging ledges of 3–15 mm in steps of 2 mm. Ledges experiment was investigated in order to identify when supports need to be introduced. Simple

geometries were designed with overhanging ledges of 0.5–6 mm in steps of 0.5 mm.

### 3.1.2. Design of support structures

An experimental test was carried out in order to find values that allow obtaining the condition most suitable for easy removal and a reduction of the deformations for most geometries. A full factorial design contains all possible combinations of a set of factors. Therefore, it could be considered as the better design approach. On the other hand, this approach requires the greatest number of experimental resources [25–29]. In order to minimize the number of tests required, Taguchi's method is used in this study. In Taguchi's methodology all factors affecting the process quality can be divided into two categories: control factors and noise factors. Noise parameters are those which cannot be controlled (or hard or expensive to control under standard production conditions). The objective is to determine the best settings of those parameters (control factors) which can be controlled during the standard conditions and minimize the effect of noise parameters which causes variability in product performance [30]. An experimental scheme is designed based on $L_{36}$ orthogonal array of Taguchi technique, which consists of 36 rows corresponding to 36 experimental runs with 35 degrees of freedom. The input or control factors are fragmentation ($Fr$) and perforation ($Pr$) kept at two levels, $Z_{offsets}$, teeth height ($T_h$), teeth base interval ($T_{Bi}$) and hatching ($H$) kept at three levels (Table 1). All the supports can have a certain offset into the part in order to ensure a better contact between part and support, called in this study $Z_{offset}$. The fragmentation and perforation were considered as logical variables: if they are used, the value is 1, otherwise the value is 0. The values used for these factors are shown in Table 1.

Optimal parametric combinations can be predicted based on signal-to-noise ratio ($S/N$). Taguchi methodology requires to distinguish experimentations for which the goal is to maximize a response, named *the-larger-the-better* problems, from those whose objective is the minimization of a variable that are called *the-smaller-the-better* problems. If the objective for the response is to achieve a target or nominal value, then the $S/N$ ratio is referred to as the *nominal-the-best* problem and is defined to decrease variability around a target response value. The objective of experiment was to optimize the support parameters in SLM process to obtain a reduction of the time, the costs of production and of the deformations. Therefore, *the-smaller-the-better* problem was used and $S/N$ ratio is calculated using Eq. (1):

$$\eta_L = -10\log_{10}\left[(1/n)\sum_{i=1}^{n}y_i^2\right] \quad [\text{dB}] \qquad (1)$$

where $\eta_L$ denotes the $S/N$ ratio calculated from observed values, $y_i$ represents the experimental observed value of the *i*th experiment,
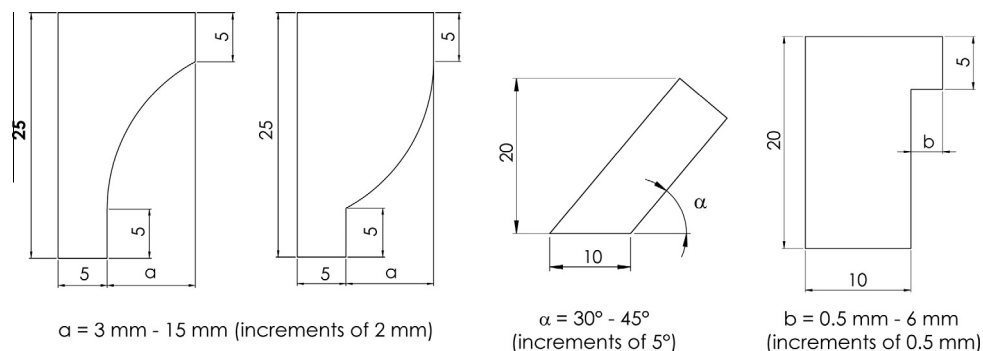


**Fig. 8.** Dimensional geometry of specimens.

**Table 1**
Support parameters value.

| Control factors | | | | |
|---|---|---|---|---|
| Parameters | Level | | | |
| | 1 | 2 | 3 | |
| Hatching (mm) | 0.5 | 0.75 | 1 | |
| Teeth height (mm) | 0.43 | 0.77 | 1.42 | |
| Teeth base interval (mm) | 0.1 | 0.3 | 0.5 | |
| $Z_{offsets}$ (mm) | 0.03 | 0.06 | | |
| Fragmentation (logic value) | 0 | 1 | | |
| Perforation (logic value) | 0 | 1 | | |
| Fragmentation | Values (mm) | | | |
| x interval | 5.6 | | | |
| y interval | 5.6 | | | |
| Separation width | 0.4 | | | |

*Perforation parameters*

| | |
|---|---|
| Style: | Diamond |
| Beam (1) : | 0.30 mm |
| Angle (2) : | 30° |
| Height (3) : | 0.5 mm |
| Solid Height (4) : | 0.254 mm |

and *n* is the number of repetition of each experiment. *The-smaller-the-better* ratio is defined to decrease variability when minimizing the response. Optimal parametric combinations can be predicted based on signal-to-noise ratio for different values. Analysis of variance (ANOVA) is then applied to calculate the statistical confidence associated with the drawn conclusions.

### 3.2. Experimental equipment and material

The AlSi10Mg and Ti6Al4V test parts were prepared by EOSINT M270 Xtended version (EOS GmbH). In this machine, a powerful Yb (Ytterbium) fiber laser system in an Ar atmosphere is used to melt powders with a continuous power up to 200 W. The detail of the SLM process, together with the choice of the process parameters to obtain a part with the highest density [31] and the best surface finishing, were described in a previous study for the aluminum alloy [32]. On the other hand, default machine process parameters were used for the titanium alloy (Table 2). Considering scanning strategy, the direction of scanning is rotated of 67° between consecutive layers. Samples dimension for analysis on the support structures were 20 × 10 × 15 mm. The support structures were created with Magics software (Materialise Company).

All test parts were built with an angle of 5° between any long edge and the recoater blade to prevent the deformation of the parts. If the long edge was parallel to the blade, this can bump over the edge causing a vibration in the build volume and can lead to powder settlement which prevents recoating on subsequent sweeps, due to the high density of the metal powder. The images of samples' surfaces are captured using the Leica EZ4 D stereo microscope. In order to compare the built parts with the CAD

**Table 2**
Process parameters values employed for aluminum and titanium alloys sample tests.

| Parameters | AlSi10Mg | | | Ti6Al4V | | |
|---|---|---|---|---|---|---|
| | Skin | Core | Contour | Skin | Core | Contour |
| Scan speed (mm/s) | 900 | 800 | 900 | 1000 | 1250 | 1250 |
| Laser power (W) | 120 | 195 | 80 | 150 | 170 | 120 |
| Hatching distance (mm) | 0.10 | 0.17 | – | 0.10 | 0.10 | . |
| Layer thickness (μm) | 30 | 30 | – | 30 | 30 | – |
| Laser spot size (mm) | 0.10 | 0.10 | 0.10 | 0.10 | 0.10 | 0.10 |

model, the samples were digitized by means of a 3D optical scanner, Atos Compact Scan 2M by GOM Gmbh.

## 4. Results and discussion

### 4.1. Self-supporting surfaces

Downward sloping face oriented at 45° showed a curl which is not significant enough to obstruct the build efficiency. Parts can be built without supports at angles up to 30° both in AlSi10Mg and Ti6Al4V alloys but the samples in aluminum have a higher surface roughness probably due to the staircase effect. The stair size decreases proportionally with the cosine of the sloping angle. As the angle decreases, the staircase effect increases, meaning that the size of each step increases. When the minimum orientation is 45°, the maximum overhanging step (layer) size was the same size as the layer thickness (30 μm). It is apparent that this is the maximum layer overhang, because greater than 30 μm caused residual curl distortion during the SLM build.

Although none of the ledges test parts collapsed, all samples showed the dross formation at down-facing surface (Fig. 9a) due to the temperature gradient mechanism [33–35]. A molten layer on top of a thin processed layer will tend to warp the previous layer towards the laser beam, because the melt pool shrinks during cooling down. The resulting complex shape depends on the anchoring of the overhang (Fig. 9b). The phenomenon is a consequence of the layer wise building with complete melting. Two possible solutions are anchoring and compensation. Anchoring the part with more support structures requires the removal of these support structures afterwards. Compensation means designing the part with a negative warping, as to obtain a flat surface after warping, which is extremely complex in any real situation. Without anchoring of the edges or corners, the warping will always hamper the proper deposition of a new layer at some stage.

Regarding the concave radii, in the top of the radius, the tangent decreases to 0° as the part grows in the z-axis, resulting in excessive layer individual overhangs. It was identified that as the tangent angle α (Fig. 10a) increases, the warping distortion decreases and the accuracy of the curve was improved (Fig. 10e).

In Fig. 10b, it is possible to see that titanium has a higher definition than aluminum (Fig. 10c). The pieces with a greater overhang of 9 mm have presented problems in construction
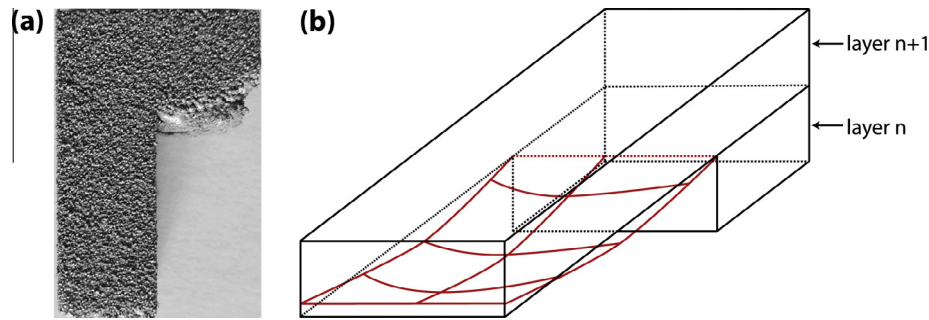
**Fig. 9.** (a) Ledges test part and (b) temperature gradient mechanism for the ledges part.
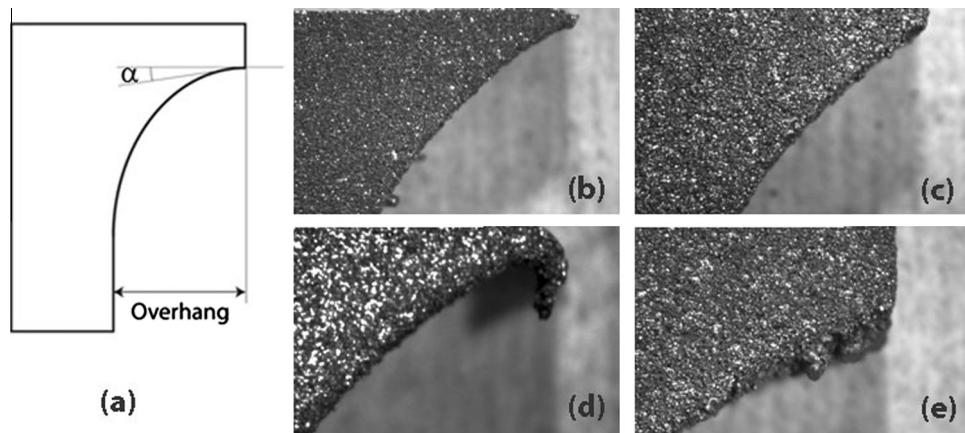


**Fig. 10.** (a) Concave radii. Titanium: (b) overhang of 9 mm, (d) overhang of 15 mm. Aluminum: (c) overhang of 9 mm, (e) overhang of 15 mm.
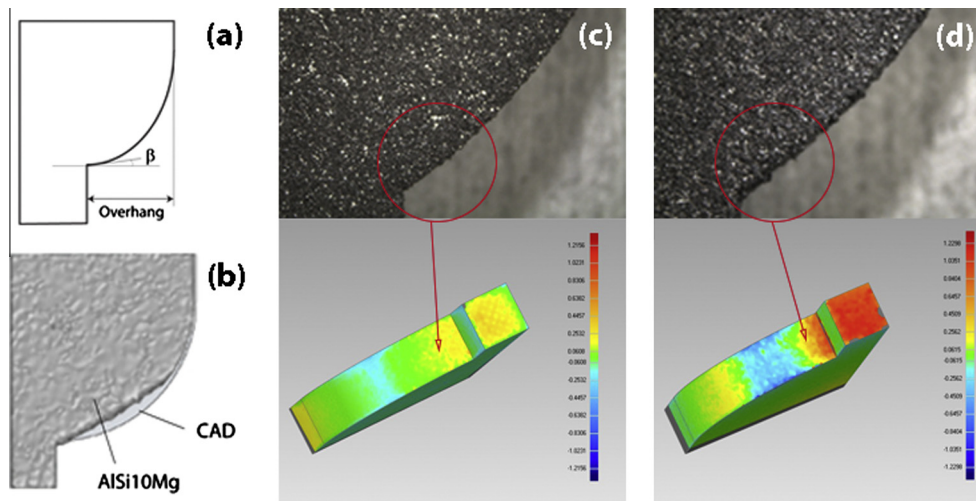


**Fig. 11.** (a) Convex radii and (b) overhang of 15 mm. Overhang of 9 mm: (c) titanium and (d) aluminum.

compared to the aluminum ones. In fact, the aluminum parts, although with the deformations of the radius of curvature, are not collapsed unlike of the pieces in titanium (Fig. 10d).

The lowest point of a traditional convex radius is vulnerable to warp. The titanium samples with an overhang of 15 mm are collapsed unlike of the aluminum samples. However, the accuracy of the radii in the aluminum sample is poor (Fig. 11b) and the radius did not resemble the original CAD data for tangent angle $\beta$ (Fig. 11a) lower than 40°. In Fig. 11, it is possible to see that titanium sample (Fig. 11c) has a higher definition than aluminum

sample (Fig. 10d) for the convex radii sample: maximum distance between CAD model and the built part is of 1.23 mm for aluminum (red[1] color in Fig. 11d), instead the distance maximum is 0.90 mm for titanium The standard deviation of the part respect to the CAD model is 0.1654 for titanium and 0.223 for aluminum.

---

[1] For interpretation of color in Fig. 11, the reader is referred to the web version of this article.

**Table 3**
Set of experiments and results.

| N | $Fr$ | $Pr$ | $Z_{offsets}$ (mm) | $T_h$ (mm) | $T_{Bi}$ (mm) | $H$ (mm) | Warp AlSi10Mg | Warp Ti6Al4V | Easy of removal AlSi10Mg | $S/N_{AlSi10Mg}$ (dB) | $S/N_{Ti6Al4V}$ (dB) |
|---|---|---|---|---|---|---|---|---|---|---|---|
| 1 | 0 | 0 | 0.03 | 0.43 | 0.10 | 0.5 | 1 | 1 | – | 0.00 | 0.00 |
| 2 | 0 | 0 | 0.03 | 0.77 | 0.30 | 0.75 | 1 | 1 | – | 0.00 | 0.00 |
| 3 | 0 | 0 | 0.03 | 1.42 | 0.50 | 1.00 | 3 | 2 | x | −9.54 | −6.02 |
| 4 | 0 | 0 | 0.06 | 0.43 | 0.10 | 0.50 | 1 | 1 | – | 0.00 | 0.00 |
| 5 | 0 | 0 | 0.06 | 0.77 | 0.30 | 0.75 | 1 | 1 | – | 0.00 | 0.00 |
| 6 | 0 | 0 | 0.06 | 1.42 | 0.50 | 1.00 | 3 | 3 | x | −9.54 | −9.54 |
| 7 | 0 | 0 | 0.06 | 0.43 | 0.10 | 0.75 | 1 | 1 | – | 0.00 | 0.00 |
| 8 | 0 | 0 | 0.06 | 0.77 | 0.30 | 1.00 | 1 | 3 | x | 0.00 | −9.54 |
| 9 | 0 | 0 | 0.06 | 1.42 | 0.50 | 0.50 | 1 | 3 | – | 0.00 | −9.54 |
| 10 | 0 | 1 | 0.03 | 0.43 | 0.10 | 1.00 | 1 | 1 | x | 0.00 | 0.00 |
| 11 | 0 | 1 | 0.03 | 0.77 | 0.30 | 0.50 | 1 | 1 | – | 0.00 | 0.00 |
| 12 | 0 | 1 | 0.03 | 1.42 | 0.50 | 0.75 | 3 | 3 | x | −9.54 | −9.54 |
| 13 | 0 | 1 | 0.06 | 0.43 | 0.30 | 1.00 | 2 | 2 | x | −6.02 | −6.02 |
| 14 | 0 | 1 | 0.06 | 0.77 | 0.50 | 0.50 | 2 | 3 | – | −6.02 | −9.54 |
| 15 | 0 | 1 | 0.06 | 1.42 | 0.10 | 0.75 | 1 | 3 | x | 0.00 | −9.54 |
| 16 | 0 | 1 | 0.03 | 0.43 | 0.30 | 1.00 | 2 | 2 | – | −6.02 | −6.02 |
| 17 | 0 | 1 | 0.03 | 0.77 | 0.50 | 0.50 | 1 | 3 | – | 0.00 | −9.54 |
| 18 | 0 | 1 | 0.03 | 1.42 | 0.10 | 0.75 | 2 | 3 | x | −6.02 | −9.54 |
| 19 | 1 | 0 | 0.06 | 0.43 | 0.30 | 0.50 | 1 | 4 | – | 0.00 | −12.04 |
| 20 | 1 | 0 | 0.06 | 0.77 | 0.50 | 0.75 | 3 | 2 | x | −9.54 | −6.02 |
| 21 | 1 | 0 | 0.06 | 1.42 | 0.10 | 1.00 | 3 | 3 | x | −9.54 | −9.54 |
| 22 | 1 | 0 | 0.06 | 0.43 | 0.30 | 0.75 | 2 | 1 | – | −6.02 | 0.00 |
| 23 | 1 | 0 | 0.06 | 0.77 | 0.50 | 1.00 | 3 | 3 | x | −9.54 | −9.54 |
| 24 | 1 | 0 | 0.06 | 1.42 | 0.10 | 0.50 | 2 | 3 | x | −6.02 | −9.54 |
| 25 | 1 | 0 | 0.03 | 0.43 | 0.50 | 0.75 | 1 | 1 | x | 0.00 | 0.00 |
| 26 | 1 | 0 | 0.03 | 0.77 | 0.10 | 1.00 | 3 | 3 | x | −9.54 | −9.54 |
| 27 | 1 | 0 | 0.03 | 1.42 | 0.30 | 0.50 | 2 | 3 | x | −6.02 | −9.54 |
| 28 | 1 | 1 | 0.06 | 0.43 | 0.50 | 0.75 | 1 | 1 | x | 0.00 | 0.00 |
| 29 | 1 | 1 | 0.06 | 0.77 | 0.10 | 1.00 | 1 | 2 | x | 0.00 | −6.02 |
| 30 | 1 | 1 | 0.06 | 1.42 | 0.30 | 0.50 | 3 | 4 | x | −9.54 | −12.04 |
| 31 | 1 | 1 | 0.03 | 0.43 | 0.50 | 1.00 | 3 | 2 | x | −9.54 | −6.02 |
| 32 | 1 | 1 | 0.03 | 0.77 | 0.10 | 0.50 | 1 | 1 | – | 0.00 | 0.00 |
| 33 | 1 | 1 | 0.03 | 1.42 | 0.30 | 0.75 | 2 | 2 | x | −6.02 | −6.02 |
| 34 | 1 | 1 | 0.03 | 0.43 | 0.50 | 0.50 | 1 | 2 | – | 0.00 | −6.02 |
| 35 | 1 | 1 | 0.03 | 0.77 | 0.10 | 0.75 | 1 | 3 | x | 0.00 | −9.54 |
| 36 | 1 | 1 | 0.03 | 1.42 | 0.30 | 1.00 | 3 | 4 | x | −9.54 | −12.04 |



1  no warp

2  warp

3  warp
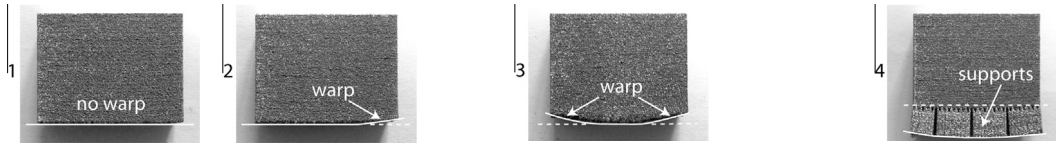
4  supports

## 4.2. Supports

The complete set of experiments is shown in Table 3. All titanium samples showed a greater ease of removal from the platform with respect to the aluminum pieces. For this reason, only for aluminum samples, a column was inserted with the result on the difficulty (–) or ease (x) to detach the samples of the building platform. The difficulty or the ease to detach a sample are measured by the time necessary to remove it from the platform: easy corresponds to less than 3 min, difficult to more than 5 min. However, the titanium samples show a higher warping effect. The $S/N$ ratio can be a positive or negative number depending on whether the mean square deviation is a number greater or smaller than 1.

**Table 5**
Analysis of Variance for AlSi10Mg. $R^2$ = 68.74%.

| Source | DOF | Seq SS | F | p | Statistical significance |
|---|---|---|---|---|---|
| $Fr$ | 1 | 1.7778 | 4.27 | 0.049 | Significant |
| $Pr$ | 1 | 0.1111 | 0.30 | 0.588 | Not significant |
| $Z_{offsets}$ | 1 | 0.0139 | 0.03 | 0.856 | Not significant |
| $T_h$ | 2 | 5.7222 | 6.88 | 0.004 | Highly significant |
| $T_{Bi}$ | 2 | 2.0556 | 2.47 | 0.104 | Not significant |
| $H$ | 2 | 5.7222 | 6.88 | 0.004 | Highly significant |
| Error | 26 | 10.8194 | | | |
| Total | 35 | 26.2222 | | | |

**Table 4**
Average $S/N_{AlSi10Mg}$ ratios.

| Level | Smaller-the-better – $S/N$ | | | | | |
|---|---|---|---|---|---|---|
| | $Fr$ | $Pr$ | $Z_{offsets}$ | $T_h$ | $T_{Bi}$ | $H$ |
| 1 | −2.928 | −4.184 | −3.989 | −2.300 | −2.594 | −2.300 |
| 2 | −5.049 | −3.793 | −3.989 | −2.887 | −4.099 | −3.096 |
| 3 | | | | −6.778 | −5.273 | −6.570 |
| Delta | 2.121 | 0.391 | 0.000 | 4.478 | 2.679 | 4.269 |
| Rank | 4 | 5 | 6 | 1 | 3 | 2 |

**Table 6**
Average $S/N_{Ti6Al4V}$ ratios.

| Level | Smaller-the-better – $S/N$ | | | | | |
|---|---|---|---|---|---|---|
| | $Fr$ | $Pr$ | $Z_{offsets}$ | $T_h$ | $T_{Bi}$ | $H$ |
| 1 | −5.245 | −5.579 | −5.522 | −3.010 | −5.273 | −6.485 |
| 2 | −6.860 | −6.526 | −6.582 | −5.775 | −6.106 | −4.184 |
| 3 | | | | −9.372 | −6.778 | −7.488 |
| Delta | 1.616 | 0.947 | 1.060 | 6.362 | 1.505 | 3.304 |
| Rank | 3 | 6 | 5 | 1 | 4 | 2 |

The response tables (Tables 4 and 6) show the average $S/N$ ratio at each level of each factor, computed from the results in Table 4. The table includes ranks based on Delta statistics, which compare the relative magnitude of effects. The Delta statistic is the highest minus the lowest average for each factor. The main effects plot (Fig. 12 and 14) provides a graph of the averages in the response table calculated for *the-smaller-the-better* case. In order to investigate the effects of supports parameters for warping defect of the part, a statistical analysis based on ANOVA is performed (Tables 5 and 7).

### 4.2.1. AlSi10Mg

The factor with the biggest impact on the $S/N$ ratio is teeth height ($T_h$), (Delta = 4.478, Rank = 1) followed by hatching ($H$), teeth base interval ($T_{Bi}$), fragmentation ($Fr$), perforation ($Pr$) and $Z_{offsets}$. Looking at the response tables and main effects plot for $S/N$ ratio, it is possible to see that teeth height and hatching have almost the same Delta (4.478 and 4.269). Therefore, one can say that they are the parameters that mostly influence the warping defect. $S/N$ ratio is minimized when the hatching is 0.5 mm, the teeth height is 0.43 mm, and the teeth base interval is 0.10 mm, fragmentation deselected and perforation selected. There is not difference between the $Z_{offsets}$ values.

Table 5 shows the ANOVA results. All factors with a $p$ value less than 0.05 are significant. Hatching, fragmentation and teeth height

have the highest relative contribution on all the performance criteria if compared to the other supports parameters.

Fig. 13 shows the interaction plot for $S/N$ ratio. Parallel lines in an interactions plot indicate no interaction. The greater the departure of the lines from being parallel, the higher the degree of interaction. If the fragmentation is not selected, a less warp occurs when the perforation is selected, $Z_{offset}$ is 0.03 mm, teeth height is 1.42 mm, teeth base interval is 0.5 mm and hatching is 1 mm. Only when teeth base interval is 0.5 mm and the fragmentation is selected, it is preferable that the supports have an offset into the part of 0.06 mm. The perforation is to be considered only in the case where teeth height is of 1.42 mm, teeth base interval is of 0.3 mm and hatching is of 1 mm.

### 4.2.2. Ti6Al4V

Fig. 14 shows the $S/N$ ratio curves for Ti6Al4V samples calculated for *the-smaller-the-better* problem. The response table (Table 5) shows that the factor with the biggest impact on the $S/N$ ratio is again teeth height ($T_h$), followed by hatching ($H$), fragmentation ($Fr$), teeth base interval ($T_{Bi}$), $Z_{offsets}$, and perforation ($Pr$). Respect to AlSi10Mg data, teeth height has a Delta greater than the hatching (6.362 and 3.304). These parameters have most influence on the warping defect. $S/N$ ratio is minimized when the hatching is 0.75 mm, the teeth height is 0.43 mm, the teeth base interval is
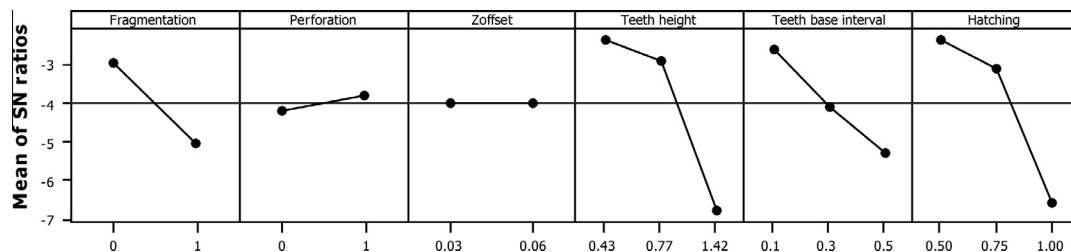


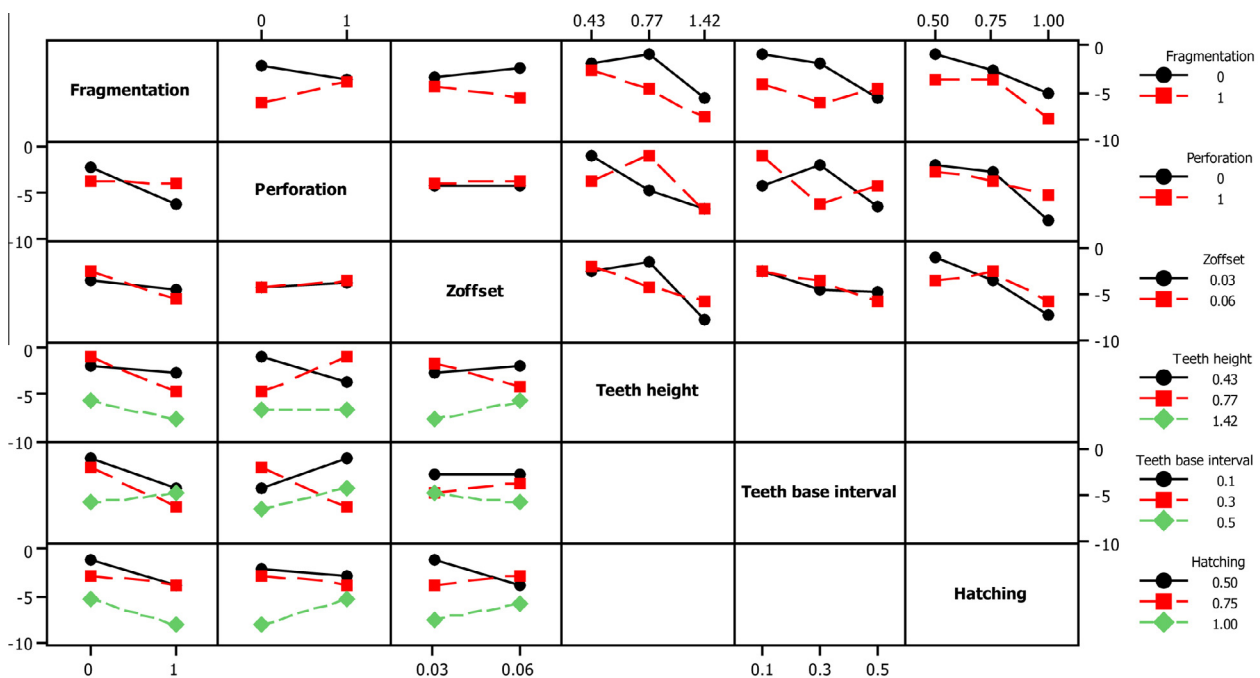**Fig. 12.** Main effects plot for $S/N_{AlSi10Mg}$ ratio. Signal-to-noise: smaller is better.



**Fig. 13.** Interaction plot for $S/N_{AlSi10Mg}$ ratio. Signal-to-noise: smaller is better.
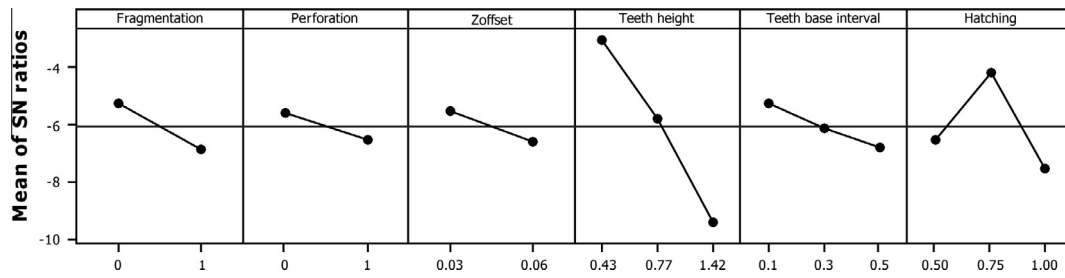
**Fig. 14.** Main effects plot for $S/N_{Ti6Al4V}$ ratio. Signal-to-noise: smaller is better.

**Table 7**
Analysis of variance for Ti6Al4V. $R^2$ = 63.44%.

| Source | DOF | Seq SS | F | p | Statistical significance |
|---|---|---|---|---|---|
| $Fr$ | 1 | 1.3611 | 2.19 | 0.151 | Not significant |
| $Pr$ | 1 | 0.2500 | 1.09 | 0.305 | Not significant |
| $Z_{offsets}$ | 1 | 1.1250 | 1.81 | 0.190 | Not significant |
| $T_h$ | 2 | 12.1667 | 9.78 | 0.001 | Highly significant |
| $T_{Bi}$ | 2 | 0.5000 | 0.40 | 0.673 | Not significant |
| $H$ | 2 | 3.1667 | 2.54 | 0.098 | Significant |
| Error | 26 | 16.1806 | | | |
| Total | 35 | 34.7500 | | | |

0.10 mm, fragmentation and perforation deselected, $Z_{offsets}$ is 0.03 mm (Table 6).

The ANOVA results show that only teeth height and hatching have a relative contribution on all the performance criteria if compared to the other supports parameters (Table 7).

Fig. 15 shows the interaction plot for $S/N$ ratio. Fragmentation is significant when the hatching is 1 mm, teeth base interval is 0.3 mm, teeth height is 1.42 mm, $Z_{offset}$ is 0.06 mm and perforation deselected. It is possible to see that perforation increases the warp for a hatching of 0.75 mm while the decreases for hatching of 1 mm. Generally, high values of the teeth height increase the warping defect with or without fragmentation and perforation. It is interesting in seeing the sharp change in slope of the curves of

fragmentation selected, no perforation and $Z_{offset}$ of 0.06 mm compared to the hatching. The value of 0.75 mm becomes a minimum point.

## 5. Optimized solutions

The part's orientation can be adjusted to improve the quality of the overhanging features. The purpose to adjust part's orientation is to alter the inclined angles of overhanging surface so as to minimize the amount of support structures as much as possible. According to the experiment on self-supporting structures, overhanging surfaces inclined at angles less than 30° require supports, while surfaces with angles between 45 and 30° are self-supported but the AlSi10Mg samples showed a high surface roughness. Although the best positions are parallel or vertical angles relative to the building platform, unfortunately these two positions do not always make it possible to build parts of complex geometry as objects with internal channels or joints. As shown in the flow-chart in (Fig. 16), to determine the optimal orientation, it is necessary to identify the surface type. In any building orientation, the part is defined with its base on the $xy$-plane and the building direction is along the $z$ axis. For a given plane, let $\vec{n}$ be its outward normal, $\vec{k}$ be the unit directional normal of a slicing plane ($z$ axis, i.e. $\vec{k}$ =[0,0,1]) and the angle $\vartheta$ be the angle between the two vectors. Therefore, considering the dot product of the two vectors,
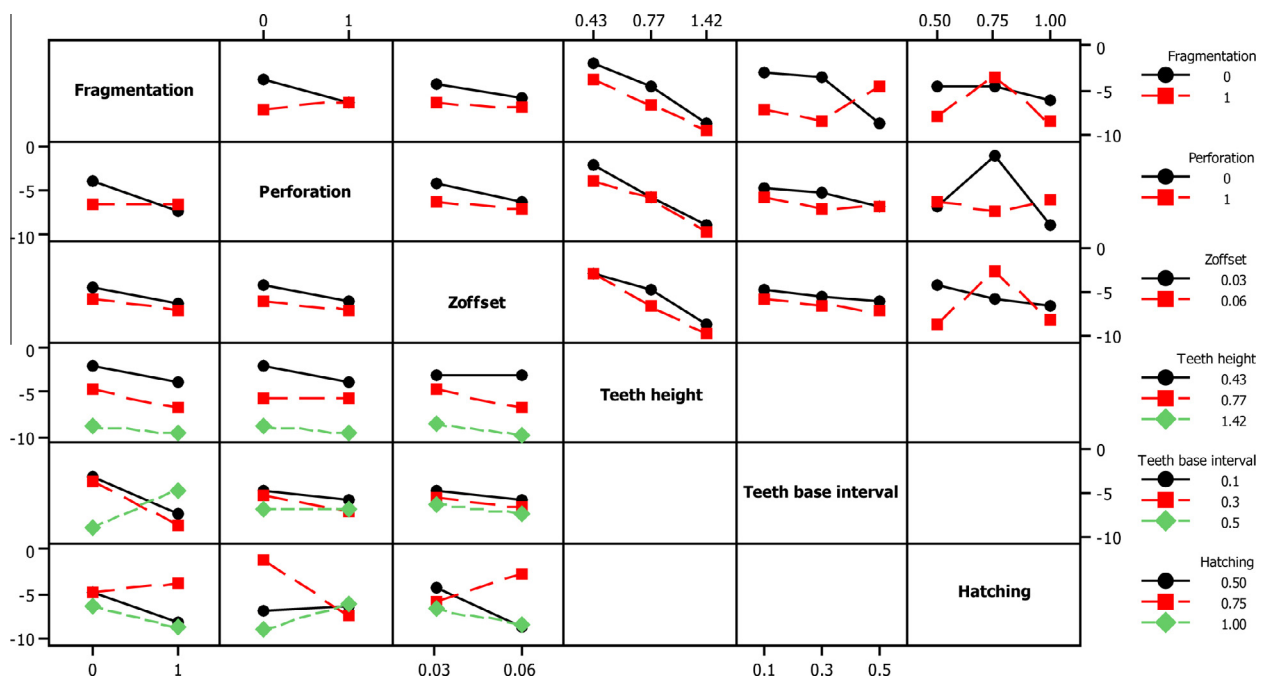


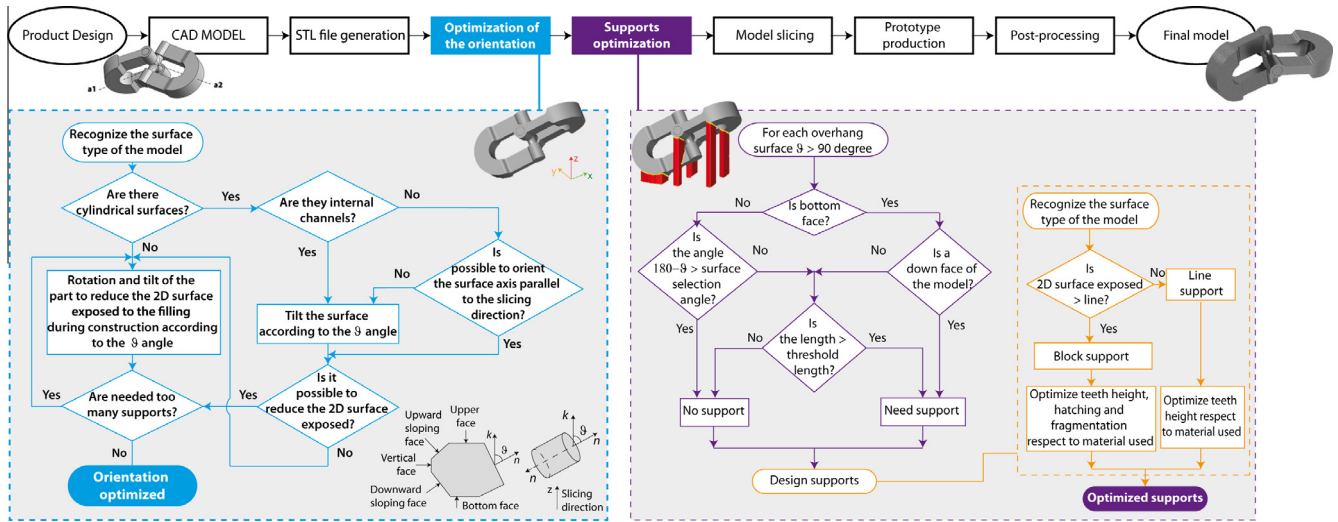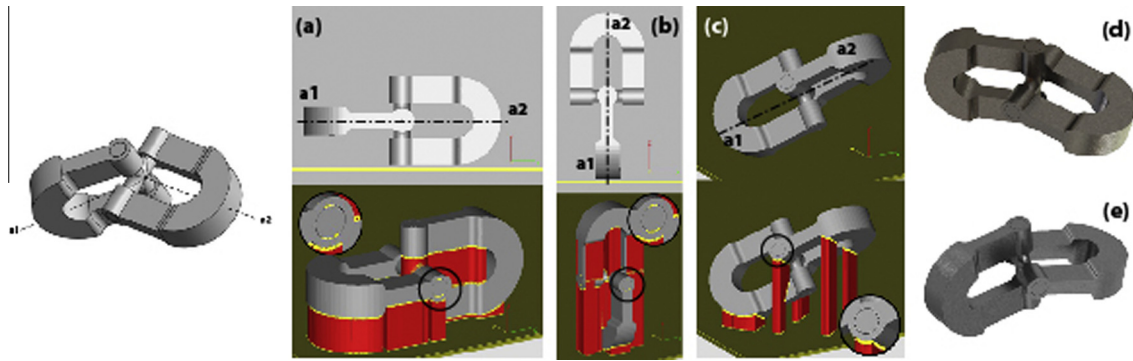**Fig. 15.** Interaction plot for $S/N_{Ti6Al4V}$ ratio. Signal-to-noise: smaller is better.

**Fig. 16.** The flowchart of the procedure.



**Fig. 17.** Effects of part's orientation on a SLM manufactured non-assembly mechanism. The *a*1-axis and *a*2-axis are (a) parallel to the building platform, (b) perpendicular to the building platform, (c) inclined with respect to the *x*-axis and *y*-axis. Samples: (d) AlSiMg alloy and (e) Ti64 alloy.

$$\vec{n} \cdot \vec{k} = |\vec{n}||\vec{k}| \cos \vartheta,$$

the following types of flat surface are analyzed:

- $\vec{n} \cdot \vec{k} = 0$ ($\vartheta = 90°$), for a vertical surface.
- $\vec{n} \cdot \vec{k} = 1$ ($\vartheta = 0°$), for a horizontal surface.
- $\vec{n} \cdot \vec{k} = -1$ ($\vartheta = 180°$), for a bottom horizontal surface.
- $0 < \vec{n} \cdot \vec{k} < 1$ ($\vartheta \leqslant 90°$), for an upward sloping surface.
- $-1 < \vec{n} \cdot \vec{k} < 0$ ($\vartheta > 90°$), for a downward sloping surface.

For a cylindrical surface:

- $\vartheta = 90°$: a cylinder or hole with the axis perpendicular to the slicing direction.
- $\vartheta \neq 90°$: a cylinder or hole tilting at an angle to the slicing direction.

It is also necessary to distinguish between overhang areas requiring supports and the roughness of the slanting surfaces due to the staircase effect. As shown in the flowchart in (Fig. 16), besides classifying the surface types, it is necessary to identify the surface type which need support structures. Based on the evaluation of several parameters, e.g. overhang, surface area, slenderness, contour length, etc., surfaces requiring support structures and support types can be determined. Fig. 17 shows a Cardan U-joint used as example in order to illustrate the procedure adopted.

Considered as an example of complex shape, this joint is a non-assembly mechanism thought and designed to be fabricated through the additive manufacturing technologies. The joint clearances of mechanisms are always very small and during SLM fabrication, the trapped powdered material and the added supports within clearance may lead to a failing fabrication. In Fig. 17, building direction (a) has the smallest *z*-directional height, so the fabrication time will be the shortest. However, this orientation needs of supports that are very difficult to remove within the small clearance. Placing direction (b) needs the least amount of external supports, but it has the biggest *z*-directional height, so longest forming time will be needed. Moreover, as building orientation (a), the joint clearances have needed the supports. So, the position (c) could be the optimal one, where the axes *a*1 and *a*2 are inclined by an angle α with respect to the axes *x* and *y*. Considering the placing orientation (c), the angle assembly of the mechanism can be adjusted for more orientations by moving the parts along the unconstrained degree of freedom, which make it possible to approach a configuration with no supports within the clearance. Moreover, this orientation also has smaller *z*-directional height than orientation (b).

Fig. 17d and e shows the samples fabricated using the orientation (c), where the angle of construction chosen allowed to build the joint without inserting supports in clearance of 0.08 mm. Moreover, the use of optimized supports has avoided distortion of the joint and made it possible to easily remove the supports.

The Cardan U-joint can be swung directly and smoothly after supports removal.

## 6. Conclusions

In this paper, an overview was given about the production of overhanging structures. Down-facing surfaces such as ledges, convex and concave radii are common features that promote a sag part deformation due to the gravity and capillary force. As a consequence, it leads to the dimensional accuracy and the shape of the SLM parts could not meet the demands. During the build of a SLM component, rapid melting and rapid cooling of the metal occurs at localized areas. The contraction of the material when cooling causes non-self-supporting material to curl away from the powder surface. The analysis found that: the downward sloping faces can be built without supports at angles up to 30° but they have a higher surface roughness; none of the ledges test parts were collapsed but all samples had distortions in the flatness of the bottom face. Regarding the concave radii, the titanium pieces with a greater overhang of 9 mm have presented problems in construction compared to the aluminum ones; and the lowest point of a traditional convex radius is vulnerable to warp. The titanium samples with an overhang of 15 mm are collapsed unlike of the aluminum samples. So, support structures can be used to prevent the deformation and/or collapse of the part during the fabrication of these overhanging structures. The presence of support structures increases both the time required for the part manufacturing and the time and complexity of post-processing operations. Minimizing the amount of supported surfaces can improve the process efficiency. For this reason, Taguchi method was used in order to find values that allow obtaining the condition most suitable for easy removal and a reduction of the deformations for most geometry. From the set of experimental investigations, the following main outcomes are obtained. For aluminum alloy, the supports are optimized when the hatching is 0.5 mm, the teeth height is 0.43 mm, and the teeth base interval is 0.10 mm, fragmentation deselected and perforation selected. There is not difference between the $Z_{offsets}$ values. For titanium alloy, the supports could be design with the hatching of 0.75 mm, the teeth height of 0.43 mm, the teeth base interval of 0.10 mm, fragmentation and perforation deselected, $Z_{offsets}$ of 0.03 mm.

Finally, the fabrication of non-assembly mechanisms by SLM in aluminum and titanium alloys was investigated and demonstrated used the optimized support structures to reduce the deformation of the overhanging surfaces. It was shown that, depending of the object built orientation, the surface area of support structures change sensitively. Therefore, it could be concluded that the orientation of the part must be considered at all stages, because it allows to reduce the number of supports avoiding the deformation of the part.

## References

[1] Strano G, Hao L, Everson RM, Evans KE. Surface roughness analysis, modelling and prediction in selective laser melting. J Mater Process Technol 2013;213:589–97.
[2] Wohlers T. Additive manufacturing and 3D printing state of the industry: Wohlers report. Fort Collins, CO, USA: Wohlers Associates Inc.; 2013.
[3] Van Bael S, Kerckhofs G, Moesen M, Pyka G, Schrooten J, Kruth JP. Micro-CT-based improvement of geometrical and mechanical controllability of selective laser melted Ti$_6$Al$_4$V porous structures. Mater Sci Eng A 2011;528:7423–31.
[4] Cooper DE, Stanford M, Kibble KA, Gibbons GJ. Additive Manufacturing for product improvement at red bull technology. Mater Des 2012;41:226–30.
[5] Song B, Dong S, Zhang B, Liao H, Coddet C. Effects of processing parameters on microstructure and mechanical property of selective laser melted Ti$_6$Al$_4$V. Mater Des 2012;35:120–5.
[6] Yan C, Hao L, Hussein A, Young P, Raymont D. Advanced lightweight 316L stainless steel cellular lattice structures fabricated via selective laser melting. Mater Des 2014;55:533–41.
[7] Allen S, Dutta D. On the computation of part orientation using support structures in layered manufacturing. In: Solid freeform fabrication symposium. Texas, USA: Austin; 1994.
[8] Frank D, Fadel G. Expert system-based selection of the preferred direction of build for rapid prototyping processes. J Intell Manuf 1995;6(5):339–45.
[9] Strano G, Hao L, Everson RM, Evans KE. A new approach to the design and optimisation of support structures in additive manufacturing. Int J Adv Manuf Technol 2013;66(9–12):1247–54.
[10] Phadke MS. Quality engineering using robust design. Prentice Hall; 1989.
[11] Park S. Robust design and analysis for quality engineering. Chapman & Hall; 1996.
[12] Yang HJ, Hwang PJ, Lee SH. A study on shrinkage compensation of the SLS process by using the Taguchi method. Int J Mach Tools Manuf 2002;42:1203–12.
[13] Kruth JP, Mercelis P, Van Vaerenbergh J, Craeghs T, Bartolo PJ, et al. Feedback Control Select Laser Melt 2008:521–7.
[14] Wang D, Yang Y, Yi Z, Su X. Research on the fabricating quality optimization of the overhanging surface in SLM process. Int J Adv Manuf Technol 2013;65(9–12):1471–84.
[15] Venuvinod PK, Ma W. Rapid prototyping – laser-based and other technologies. Kluwer Academic Publishers 2003. ISBN: 1-4020-7577-4.
[16] Pauwels J, Swaelens B, Vancraen W. Method for supporting an object made by means of stereolithography or another rapid prototype production method. Patent US5595703 A; 1997.
[17] Venuvinod PK, Ma W. Rapid prototyping: laser-based and other technologies. US: Springer; 2004.
[18] Hussein A, Hao L, Yan C, Everson R, Young P. Advanced lattice support structures for metal additive manufacturing. J Mater Process Technol 2013;213:1019–26.
[19] Chen YH, Chen ZZ. Joint analysis in rapid fabrication of non-assembly mechanisms. J Rapid Prototyping 2011;17:408–17.
[20] Yang Y, Su X, Wang D, Chen Y. Rapid fabrication of metallic mechanism joints by selective laser melting. Proceedings of the Institution of Mechanical Engineers, Part B: Journal of Engineering Manufacture 2011;225:2249.
[21] Kruth JP, Vandenbroucke B, Van Vaerenbergh P. Benchmarking of different sls/slm processes as rapid manufacturing technologies. In: International conference of polymers and moulds innovations (PMI), Gent; April 2005.
[22] Vandenbroucke B, Kruth JP. Selective laser melting of biocompatible metals for rapid manufacturing of medical parts. Rapid Prototyping J 2007;13(4):196–203.
[23] Rehme O, Emmelmann C. Rapid manufacturing of lattice structures with SLM. Proceed. SPIE 2006;6107:192–203.
[24] Thomas D. The development of design rules for Selective Laser Melting. Ph.D. Thesis, University of Wales Institute, Cardiff; 2009.
[25] Antony J. Taguchi or classical design of experiment: a perspective from a practitioner. Sens Rev 2006;26:227–30.
[26] Yusoff N, Ramasamy M, Yusup S. Taguchi's parametric design approach for the selection of optimization variables in a refrigerated gas plant. Chem Eng Res Des 2011;8:665–75.
[27] Roy RK. A primer of taguchi method. New York: van Nostrand Reinhold; 1990.
[28] Youssef YA, Beauchamp Y, Thomas M. Comparison of a full factorial experiment to fractional and taguchi designs in a lathe dry turning operation. Comput Ind Eng 1994;27:59–62.
[29] Ballantyne KN, Van Oorschot RA, Mitchell RJ. Reduce optimisation time and effort: Taguchi experimental design methods. Forensic Sci Int: Genetics Suppl Series 2008;1:7–8.
[30] Van Elsen M. Complexity of selective laser melting: a new optimisation approach. PhD Thesis; 2007.
[31] Manfredi D, Calignano F, Krishnan M, Canali R, Ambrosio EP, Atzeni E. From powders to dense metal parts: characterization of a commercial AlSiMg alloy processed through direct metal laser sintering. Materials 2013;6:856–69.
[32] Calignano F, Manfredi D, Ambrosio EP, Iuliano L, Fino P. Influence of process parameters on surface roughness of aluminum parts produced by DMLS. Int J Adv Manuf Technol 2013;67(9–12):2743–51.
[33] Kruth JP, Froyen L, Van Vaerenbergh J, Mercelis P, Rombouts M, Lauwers B. Selective laser melting og iron based powder. J Mater Process Technol 2004;149(1–3):616–22.
[34] Zaeh MF, Ott M. Investigations on heat regulation of additive manufacturing processes for metal structures. CIRP Annals-Manuf Technol 2011;60:259–62.
[35] Matsumoto M, Shiomi M, Osakada K, Abe F. Finite element analysis of single layer forming on metallic powder bed in rapid prototyping by selective laser processing. Int J Mach Tools Manuf 2002;42(1):61–7.